Particle Accelerators, 1997, Vol. 56, pp. 147–160
Reprints available directly from the publisher
Photocopying permitted by license only

NEW THEORETICAL DESIGNS FOR DIPOLE MAGNETS

K.V. BHAGWAT[a] and P. CHADDAH[b]

[a]*Solid State Physics Division, Bhabha Atomic Research Centre, Bombay 400085, India*
[b]*Low Temperature Physics Group, Centre for Advanced Technology, Indore 452013, India*

(Received 12 April 1995; in final form 7 August 1996)

We present a new class of theoretical designs for cylindrical magnets of circular cross-section that analytically yield a constant field in the inner bore. We suggest an optimized design and compare it with the conventional $\cos\theta$ design. The new design has two attractive features. The bore is elliptic in shape with the long axis along the field direction. Further, it has a smaller outer diameter compared with the $\cos\theta$ design for a given dipole field and peak current density and for a given bore dimension perpendicular to the field axis. We also discuss a scheme for winding a magnet approximating our design.

Keywords: Electromagnetic field calculations; magnetic fields; magnets.

1 INTRODUCTION

Cylindrical superconducting magnets are used in high-energy storage rings to generate a constant field perpendicular to the cylinder axis inside their inner bore. Standard text books[1,2] on magnet design discuss two designs for a dipole magnet, viz., the "$\cos\theta$" design and the "intersecting ellipses" design. A recent article by Schmuser[3] presents a detailed review on these two designs. The outer cross-section of the magnet is circular and a bore of the same shape, in the case of the $\cos\theta$ design and a more complicated shape in the intersecting ellipses design. These designs are based on their theoretical versions which *analytically* yield a uniform field in the bore region of the magnet. In this paper we present a new class of theoretical designs for a dipole magnet having a circular outer cross-section and an elliptical bore that

also *analytically* yield a constant field in its interior. Thus the well-known $\cos\theta$ design is just one member of this class. Each design of the class is characterized by an arbitrary function which determines the eccentricity of the cross-section of the bore. This function may be optimized to suit the desired special requirements. We assume that the maximum current density that can be passed through the conductor, the desired bore field value and the bore dimension perpendicular to the field axis are specified. We then provide an optimum design which has a smaller outer diameter (by up to 17%) compared to the conventional $\cos\theta$ design.

The present design is motivated by our recent work on Bean's Critical State model for hard type-II superconductors as applied to sample shapes with nonzero demagnetization factors.[4–7] Amongst the sample shapes we have considered is that of an infinite cylinder, of elliptic cross-section in an applied field $H_a\mathbf{j}$ along one of its principal axes. Both the cartesian and polar axes used in this paper are shown in Figure 1. The induced currents set up under application of an external field $H_a\mathbf{j}$ are $\mathbf{J}(r,\theta) = J(r,\theta)\mathbf{k}$, where $\mathbf{k}$ is a unit vector along the cylinder axis and the function $J(r,\theta)$ satisfies $J(r,\theta+\pi) = -J(r,\theta)$. For an infinite cylinder with currents parallel to the cylinder axis one cannot distinguish between induced currents (as in the Critical State) and transport currents (as in a magnet). We shall now refer to $J(r,\theta)$ as transport currents and use the mathematical formalism of our earlier work.[4–7] Assuming that these currents flow between the outer surface and an inner surface (called the flux front) $r = f(\xi_0,\theta)$, where ξ_0 is a parameter related to the magnitude of H_a, we have solved[4] for $f(\xi,\theta)$ and $J(r,\theta)$, such that $\mathbf{B} = 0$ in the interior of the flux front. If we denote by $\mathbf{B}_J(r,\theta)$, the field generated by the current distribution then this implies that $\mathbf{B}_J(r,\theta) = -H_a\mathbf{j}$ in the interior of the flux front. Our solutions for $J(r,\theta)$ and $f(\xi,\theta)$ thus provide a set of designs for cylindrical dipole magnets of elliptical outer cross-section and which generate a constant field (along $\mathbf{j}$) in their interior.

In this paper, however, we restrict ourselves to the case of cylindrical magnets with circular outer cross-section. In Section 2 we present general results for $J(r,\theta)$ and $f(\xi,\theta)$ that generate a constant field $B_0\,\mathbf{j}$ in the inner bore, i.e., the interior of $r = f(\xi_0,\theta)$ (see Figure 1). We then choose that solution which leads to the largest possible dimension of the inner bore along the x-axis. This is our optimum design which is the main concern of this paper. In Section 3 we compare our design with the $\cos\theta$ design. In Section 4 we consider the implementation of the optimum design and discuss possible schemes for practically winding a magnet of our design.

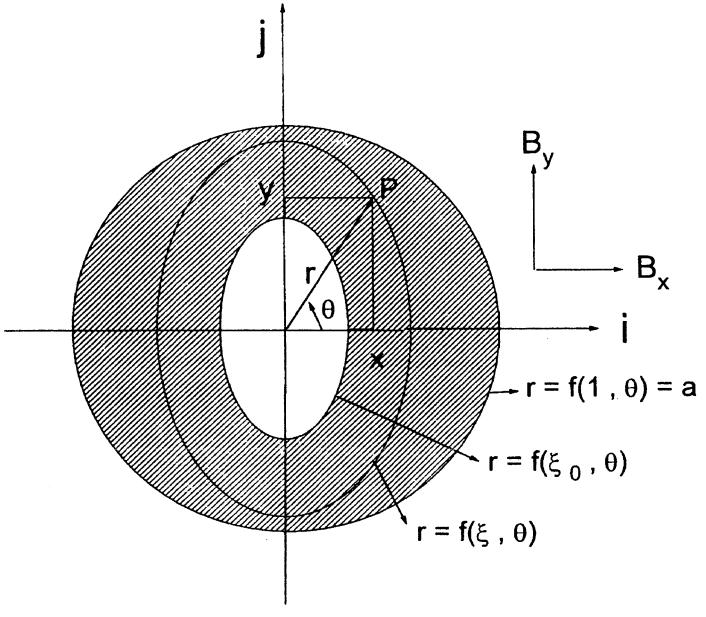

FIGURE 1 The cartesian and polar axes used are depicted. The unit vectors **i** and **j** are along the cartesian axes X and Y respectively. The magnet axis is along the unit vector **k** perpendicular to the plane of the figure. $r = a$ is the outer circular cross-section of the magnet, while $r = f(\xi_0, \theta)$ is the cross-section of the inner bore. The parameter ξ_0 is the ratio of the transverse bore dimension to the outer radius. The shaded region carries the current density $J(r, \theta)$. Flux-fronts like $r = f(\xi, \theta)$, $\xi_0 \leq \xi \leq 1$ scan the entire current carrying region. The magnetic induction **B** has two components B_x and B_y and $B_x = 0$ within the bore.

2 DIPOLE MAGNETS OF CIRCULAR CROSS-SECTION

We consider an infinite cylinder of outer radius a and the inner bore given by $r = f(\xi_0, \theta)$, (Figure 1). The cylinder carries a current $J(r, \theta)$ parallel to the axis, and satisfies the condition $J(r, \theta + \pi) = -J(r, \theta)$. The entire current carrying region of the cylinder is spanned by $r = f(\xi, \theta)$, with ξ varying from ξ_0 to 1, and we impose the boundary condition $f(1, \theta) = a$. The current carrying region generates a field $\mathbf{B}_J(\mathbf{r})$ and we require that $\mathbf{B}_J(\mathbf{r}) = -B_0\mathbf{j}$, for **r** lying within the flux-front $f(\xi_0, \theta)$. Working in cartesian coordinates, we have

$$\mathbf{B}_J(x, y) = \frac{\mu_0}{2\pi} \int \frac{J(x', y')[-(y - y')\mathbf{i} + (x - x')\mathbf{j}}{(x - x')^2 + (y - y')^2} dx'dy' \qquad (1)$$

where the integral is over the current carrying part of the cross-section of the cylinder. Instead of working with the vector $\mathbf{B}_J$ it is advantageous[2] to work with a complex number $B(z)$

$$B^*(z) = \frac{\mu_0}{2\pi} \int \frac{J(x', y')(z - \zeta)}{|z - \zeta|^2} dx'dy' \qquad (2)$$

where $z = x + iy, \zeta = x' + iy', B_x = ImB$ and $B_y = ReB$. Since the current density is real, one can write[2]

$$B(z) = \frac{-\mu_0}{2\pi} \int \frac{J(x', y')}{(z - \zeta)} dx'dy' \qquad (3)$$

If z lies in a circular region of radius r_0 (centred about the origin) such that $r_0 < |\zeta|$ for all ζ in the current carrying region, we may expand the factor $(z - \zeta)^{-1}$ of the integrand of Equation (3) in a power series to get

$$B(z) = \frac{\mu_0}{2\pi} \sum_{n=0}^{\infty} z^n \int \zeta^{-(n+1)} J(x', y')dx'dy' \qquad (4)$$

writing $\zeta = u \exp(i\phi)$, we get

$$B(z) = \frac{\mu_0}{2\pi} \sum_{n=0}^{\infty} z^n \int u^{-n} e^{-i(n+1)\phi} J(u, \phi)dud\phi \qquad (5)$$

We now change the variable from u to ξ' by setting $u = f(\xi', \phi)$ and note that the current carrying region is spanned by varying ξ' from ξ_0 to 1. Thus we get

$$B(z) = B_0 + \frac{\mu_0}{2\pi} \sum_{n=1}^{\infty} z^n \int_{\xi_0}^{1} d\xi' \int_{-\pi}^{\pi} d\phi f^{-n} e^{-i(n+1)\phi} J(\xi', \phi) f_{\xi'} \qquad (6)$$

where we have denoted by $f_{\xi'}$, the partial derivative $\partial f/\partial \xi'$. Further, B_0 is the $n = 0$ term of Equation (5) and is independent of z. It was shown in Reference 4 and also detailed in the appendix, that if we choose

$$f(\xi, \theta) = a\xi/[1 + p(\xi)\sin^2\theta]^{1/2} \tag{7}$$

with $p(\xi)$ an arbitrary function, [This corresponds to the inner bore being an elliptical cylinder with the semi axes $a\xi_0$ (perpendicular to the field axis) and $a\xi_0/[1 + p(\xi_0)]^{1/2}$, (see Figure 1)], and choose

$$J(\xi, \theta) = aJ_c[f\cos\theta + (\partial f/\partial\theta)\sin\theta]/[f(\partial f/\partial\xi)] \tag{8}$$

then all the terms under the summation in Equation (6) vanish identically and B_0 is real. We will then have $B_x = 0$, $B_y = B_0$ in the circular cylinder of radius r_0. It follows by analytic continuation that $\mathbf{B}_J = B_0\mathbf{j}$ throughout the inner bore. It should be mentioned here that the form (8) of the current density was obtained by imposing the constraint that it generates uniform *Amperian magnetization* (resulting from Ampere's equivalent shell theorem applied to various current loops constituting the current distribution) in the bore region.[4] The details are given in the appendix. This property is exhibited also by the two afore mentioned magnet designs. An explicit calculation following Reference 2 shows that the field within the bore is indeed constant and is given by

$$B_0 = \mu_0 J_c a \int_{\xi_0}^{1} \frac{\{[1 + p(\xi)]^{1/2} - 1\}}{p(\xi)} d\xi \tag{9}$$

It is clear that in the present frame-work the $\cos\theta$ design corresponds to the choice $p(\xi) = 0$. For the optimum design we choose $p(\xi) = \xi - 1$. This maximizes ξ_0 in Equation (9) for a given value of the bore field B_0 and a fixed value of J_c.[7] Thus for a fixed transverse bore dimension $a\xi_0$ the optimum design has the smallest outer dimension a.

We now give an explicit expression for the current density relevant for the optimum design. It follows from Equations (7) and (8) with optimum $p(\xi) = \xi - 1$ that

$$J(r, \theta) = J_c\cos\theta/[\cos^2\theta + (r^2/4a^2)\sin^4\theta] \tag{10}$$

Transforming to cartesian co-ordinates we have

$$J^2(x, y) = 4[J_c^2 - J^2(x, y)](a^2x^2/y^4) \tag{11}$$

Hence $J(x, y)$ is constant along the parabola

$$y^2 = 2[J_c^2/J^2 - 1]^{1/2}ax \tag{12}$$

It may be recalled that for the conventional $\cos\theta$ design both the outer cross-section and the bore are circular in shape and $J(x, y)$ is constant along straight lines passing through the origin.

3 COMPARISON WITH $\cos\theta$ DESIGN

We note that J_c, the current density at $\theta = 0$, is determined by the conductor used and will be assumed to be specified. For a given value of a, the outer radius and a given bore dimension $2a\xi_0$ perpendicular to the field axis, we compare the dipole fields in the two designs. Using Equation (9) with optimum $p(\xi)$ we get

$$B_0[\text{opt}] = 2\mu_0 J_c a[1 - \sqrt{\xi_0} - \ln\{2/(1 + \sqrt{\xi_0})\}] \tag{13}$$

and for the $\cos\theta$ design ($p(\xi) = 0$) we get

$$B_0[\cos\theta] = (\mu_0 J_c a/2)[1 - \xi_0] \tag{14}$$

In Figure 2 we plot $(B_0/\mu_0 J_c a)$ for the two designs. Our design gives a higher value, and the difference increases as ξ_0 (or the bore size) decreases. The maximum gain in B_0 is about 22% at $\xi_0 = 0$. We can invert the argument and say that if B_0 and $a\xi_0$ are specified, the outer radius a is smaller for the optimum design. We shall come back to this point later.

The second point to recall is that the inner bore is an ellipse with the semi-major axis $b = a\xi_0/[1 + p(\xi_0)]^{1/2}$ along the field direction. For the optimum design this simply reduces to $a\sqrt{\xi_0}$ while the corresponding value for the $\cos\theta$ design is $a\xi_0$. The variation of b with ξ_0 is shown in Figure 3. The larger value of b may have an advantage when it is desired to have two vacuum chambers, one above the other, within the same magnet bore carrying different particles as for a particle-antiparticle collider.

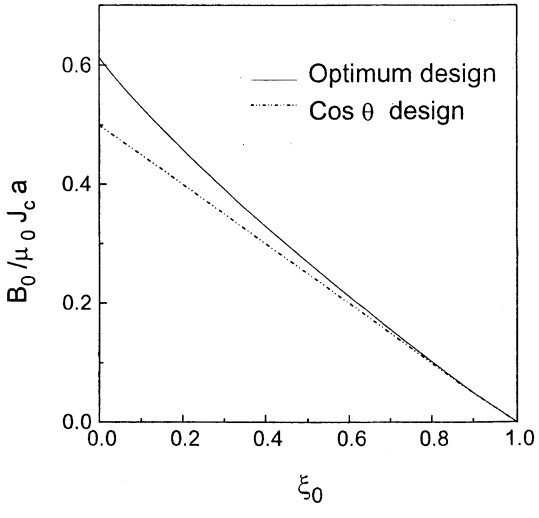

FIGURE 2 A comparison of $B_0/\mu_0 J_c a$, for various values of ξ_0 for the optimum design and the $\cos\theta$ design with the same outer dimension a.

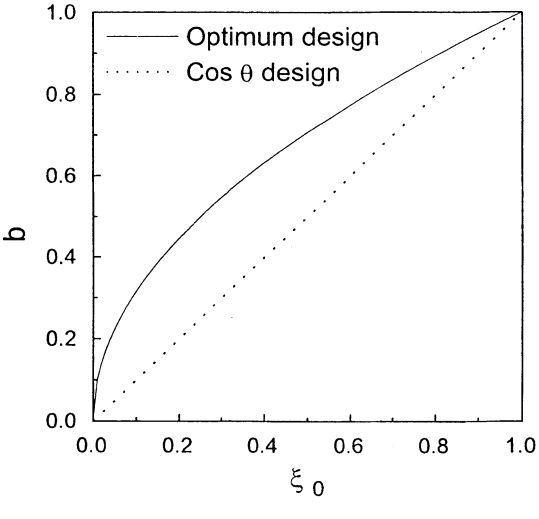

FIGURE 3 The plot of b/a, for various values of ξ_0 for the optimum design and the $\cos\theta$ design having the same outer dimension a and the same transverse bore-dimension $a\xi_0$. The dimension of the bore along the field axis is $2b$.

In practice the magnet will be wound to accommodate a beam tube with fixed dimension. Thus the size of the inner bore $a\xi_0$ and the field B_0 within the bore shall be specified. It would be worthwhile to compare the amount of conductor required, the field values at the outer surface as well as the total flux leaking out of the magnet for the $\cos\theta$ and the optimum design.

Let $a[\text{opt}]$ and ξ_0 be the outer radius and the ξ-value of the inner bore for the optimum design and $a[\cos\theta]$ and ξ_0' denote the corresponding quantities for the $\cos\theta$ design. Then we require for comparison hereafter

$$a[\text{ opt }]\xi_0 = a[\cos\theta]\xi_0' \tag{15}$$

and

$$B_0[\text{ opt }] = B_0[\cos\theta] = B_0 \tag{16}$$

From Equations (13), (14) and (15) it follows that

$$\xi_0/\xi_0' = \xi_0 + 4[1 - \sqrt{\xi_0} - \ln\{2/(1+\sqrt{\xi_0})\}] \tag{17}$$

Let R_a denote the ratio ξ_0/ξ_0' $\{= a[\cos\theta]/a[\text{ opt }]$ (cf. Equation (15))$\}$. In Figure 4 curve-B we plot R_a as function of ξ_0. It is clear that for small ξ_0(large bore field B_0), $a[\cos\theta]$ is significantly large compared to $a[\text{opt}]$.

Next we compare the volume of the conductor required for winding the magnet. The required current density may be generated by varying the conductor density keeping the source current fixed. The volume of the conductor $V[J]$ required for the current distribution $J(r,\theta)$ is then given by

$$V[J] = L\int rdrd\theta\ J(r,\theta)/J_c = 4a^2L\int_{\xi_0}^{1}\frac{\xi d\xi}{\sqrt{1+p(\xi)}} \tag{18}$$

where L is the long dimension of the magnet. A simple calculation shows that for $p(\xi) = 0$

$$V[\cos\theta] = 2a[\cos\theta]^2(1-\xi_0'^2)L \tag{19}$$

and for $p(\xi) = \xi - 1$

$$V[\text{ opt }] = (8/3)a[\text{ opt }]^2(1-\xi_0^{3/2})L \tag{20}$$

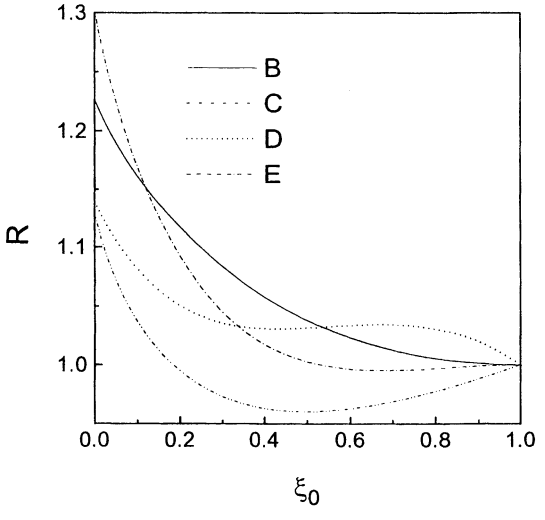

FIGURE 4 A comparison of the optimum design and the $\cos\theta$ design when both are wound with identical conductor, generate the same bore field B_0, have the same transverse bore dimension $2a\xi_0$ and are operated with a current source providing a fixed current density. The curve B compares the ratio of outer radii $a[\cos\theta]/a[\text{opt}]$. The x-axis is the ratio of the transverse inner bore dimension to the outer diameter for the optimum design. With $a\xi_0$ and J_c specified, ξ_0 decreases with increasing B_0 as follows from Figure 2. The curve C represents the ratio $V[\cos\theta]/V[\text{opt}]$ of the conductor voulmes required. The curve D represents the ratio of the fields $B[\cos\theta]/B[\text{opt}]$ at $r = a, \theta = 0$. The curve E represents the ratio $F[\cos\theta]/F[\text{opt}]$ of the total (integrated over the region exterior to the magnet) flux leaking out of the magnet.

Using relation (11) the ratio $R_v = V[\cos\theta]/V[\text{opt}]$ can be expressed as a function of ξ_0. This has been plotted in Figure 4 curve-C. The ratio R_v has its minimum value (≈ 0.96) at $\xi_0 \approx 0.5$. The optimum design requires less conductor volume (up to $\approx 8\%$) in the range of $0 \leq \xi_0 \leq 0.2$. Small value of ξ_0 corresponds to large value of the bore field.

We may also compare the fields (B_J) generated by the current distribution at a point $a\xi, \xi > 1$ in the $\theta = 0$ plane. A simple calculation[7] shows

$$B_J = \mu_0 J_c a \int_{\xi_0}^{1} \left[\frac{[1 + p(\xi')]\xi}{[\{1 + p(\xi')\}\xi^2 - p(\xi')\xi'^2]^{1/2}} - [1 + p(\xi')]^{1/2} \right] \frac{d\xi'}{p(\xi')} \tag{21}$$

For $p(\xi') = \xi' - 1$ we get $B_J[\text{opt}]$ and for $p(\xi') = 0$ we get $B_J[\cos\theta]$. The ratio $R_B = B_J[\cos\theta]/B_J[\text{opt}]$ is plotted in Figure 4 curve D. This ratio is always found to be greater than 1.

Using the expression for B_J we can compute the flux leaking out per unit length of the magnet and this is given by

$$F = \mu_0 J_c a^2 \int_{\xi_0}^{1} \frac{\xi'^2 d\xi'}{[\{1 + p(\xi')\} - p(\xi')\xi'^2]^{1/2} + [1 + p(\xi')]^{1/2}} \tag{22}$$

Using the appropriate form of $p(\xi')$ we can determine $F[\cos\theta]$ and $F[\text{opt}]$ and hence the $R_F = F[\cos\theta]/F[\text{opt}]$. In Figure 4 curve-E we have plotted R_F as a function of ξ_0. It may be noted that for $\xi_0 < 0.5$, the ratio $R_F > 1$, it attains a minimum and rises again.

4 PRACTICAL WINDING SCHEME

The current distribution we desire is given by Equation (10). This can, in principle, be realized by winding parabolic layers of identical conductor, but with different current supplies for each layer. This possibility is hard to realize in practice. A second possibility is to use a common current supply with each layer having a conductor density such that Equation (10) is satisfied.

The practical method used to wind the $\cos\theta$ design is to put insulating wedges along the cross-section of the cylinder and wind the magnet with one particular conductor carrying a uniform current. The current carrying region is divided into several zones. Each zone is further subdivided into two parts, one part with area A_c filled with conductor and the other with area A_i is filled with an insulator. A current of the same density obtained from a common source is passed through all the conducting zones. The conducting subzone carries the same *total* current as would be carried by the full zone as per the $\cos\theta$ current distribution. The number and location of the wedges is chosen so as to approximate the $\cos\theta$ distribution[1,3] for the current density as closely as required within the limits of tolerance for the nonuniformity of the bore field actually generated. This method can be adapted for our design as well. We present a schematic of the cross-section in Figure 5. Since lines of constant current density are parabolas, the various zones and subzones have

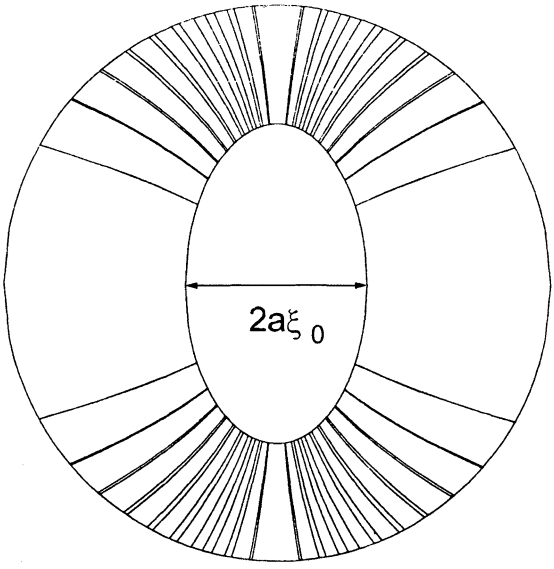

FIGURE 5 A schematic cross-section for a practical realization of the optimum design. The parabolic zones are to be alternately filled with conductor and insulator. At $\theta = 0$ there is a large conducting zone followed by a wafer thin insulating zone. The size of the conducting zone reduces and that of the insulating zone increases as θ increases. The largest insulating zone is at $\theta = \pi/2$. The wedge structure may be compared with that for the $\cos\theta$ design given in references.[1–3]

parabolic boundaries. The size of the conducting subzone decreases and that of an insulating subzone increases as θ varies (see Figure 1) from 0 to $\pi/2$.

5 CONCLUSIONS

We have presented a new class (characterized by a function $p(\xi)$) of theoretical designs for a dipole magnet. We have provided a new optimum design for a dipole magnet which will reduce the lateral size of the magnet for specific practical requirements. We have compared its features with the conventional $\cos\theta$ design. The optimum design would be particularly useful if large internal field is desired. In this field range it has low leakage field in the immediate (outer) vicinity of the magnet and also small total flux leakage.

The comparison of the optimum design with the $\cos\theta$ is only incidental. It should be remembered that the theoretical designs of the new class, in general, include magnets with elliptical — both prolate and oblate — outer cross-section. The designers of magnet may possibly choose to optimize one of these using different criteria. Finally, as noted earlier, the two well known designs for dipole magnets as well as those of the general class mentioned in this paper have one feature in common, viz., the appropriate current density that generates uniform bore field *also* generates uniform Amperian magnetization within the bore. Whether such a constraint has any deeper significance needs to be investigated.

6 APPENDIX

We present a derivation of the expression (Equation (8)) for the current density. Consider a current carrying region bounded between two cylindrical surfaces $r = f(1, \theta)$, and $r = f(\xi_0, \theta)$ ($r = \sqrt{x^2 + y^2}$) with current density J directed along the cylinder axis (z-axis). The current carrying region can be viewed as a stack of planar current loops. The Amperian magnetization at a point (x, y) within the current carrying region is given by

$$M(x, y) = \int_{x}^{x_{\max}} J du \tag{A.1}$$

The integral represents contributions from planar loops for a fixed y, and $x_{\max}$ is determined so that the point $(x_{\max}, y)$ lies on the surface $r = f(1, \theta)$. The magnetization in the bore region would be obtained by replacing the lower limit x by $x_{\min}$ such that $(x_{\min}, y)$ lies on the surface $r = f(\xi_0, \theta)$. Denoting this by M_{in} we have

$$M_{in}(x, y) = \int_{x_{\min}}^{x_{\max}} J du \tag{A.2}$$

We now change the variable of integration from $u = r\ \cos\theta$ to ξ through the substitution $r = f(\xi, \theta)$ so that $y = f(\xi, \theta)\ \sin\theta$ is held fixed. This leads to

$$M_{in}(x, y) = \int_{\xi_0}^{1} \frac{J\ f\ f_\xi\ d\xi}{(f\ \cos\theta + f_\theta \sin\theta)} \tag{A.3}$$

Thus M_{in} is independent of x, y if the integrand is a function of ξ alone. This leads to the expression

$$J(\xi, \theta) = g(\xi)[f \cos\theta + (\partial f/\partial\theta) \sin\theta]/[f(\partial f/\partial\xi)] \tag{A.4}$$

for some function $g(\xi)$. The choice $g(\xi) = aJ_c$ leads to Equation (8).

We now show that every term in the sum on the right hand side of Equation (6) vanishes identically for the choice of the flux-front and the current density as given by Equations (7) and (8). Let us denote by I_n the integral over ϕ on the right hand side of Equation (6). Thus we have for $n = 1, 2, 3, \ldots$

$$I_n = \int_{-\pi}^{\pi} f^{-n} e^{-i(n+1)\phi} J(\xi', \phi) f_{\xi'}\, d\phi \tag{A.5}$$

Equation (8) for the current density may be rewritten as

$$f_{\xi'}\ J(\xi', \phi) = [aJ_c/f(\xi', \phi)]\partial(f \sin\phi)/\partial\phi$$

Next the integrand may be treated as a product of factors $(f \sin\phi)^{-(n+1)}$ and $(\sin\phi e^{-i\phi})^{n+1}$ to facilitate integration by parts. The integrated term vanishes at both the limits and we have

$$I_n = \frac{(n+1)}{n} \int_{-\pi}^{\pi} f^{-n} e^{-i(n+2)\phi}\, d\phi \tag{A.6}$$

Since $f(\xi', -\phi) = f(\xi', \phi)$ only the cosine part of the exponential will give a non zero contribution to I_n and the range of integration can be reduced to $(0, \pi)$. Furthermore, for an odd integral value of n, $\cos n\phi$ is an odd function of ϕ about the value $\phi = \pi/2$. Hence we conclude that I_n must vanish for $n = 2k+1$, $k = 0, 1, 2, \ldots$. For even values of n, say $n = 2k$, $k = 1, 2, 3, \ldots$ use of the explicit form of f (c.f. Equation (7)) gives the following expression for I_{2k}

$$I_{2k} = \frac{(2k+1)}{k}(a\xi')^{-2k} \int_0^{\pi} [1 + p(\xi') \sin^2 \phi]^k \cos[2(k+1)\phi]\, d\phi \quad \text{(A.7)}$$

Noting the fact that

$$[1 + p(\xi') \sin^2 \phi]^k = \sum_{l=0}^{2k} \gamma_l(\xi') \cos l\phi$$

where the γ_l's are independent of ϕ, it is clear that $I_{2k} = 0$ for $k = 1, 2, 3, \ldots$ etc.

References

[1] Wilson, M.N. (1963). *Superconducting Magnets*, Oxford, Clarendon Press, pp. 27–32.
[2] Brechna, H. (1973). *Superconducting Magnet Systems*, Springer Verlag, Heidelberg Berlin, pp. 30–46.
[3] Schmuser, P. (1991). *Rep. Prog. Phys.*, **54**, 683.
[4] Bhagwat, K.V. and Chaddah, P. (1989). *Pramana J. Phys.*, **33**, 521–540.
[5] Bhagwat, K.V. and Chaddah, P. (1990). *Physica*, **C166**, 1–8.
[6] Bhagwat, K.V. and Chaddah, P. (1992). *Physica*, **C190**, 444–452.
[7] Bhagwat, K.V. and Chaddah, P. (1994). *Physica*, **C224**, 155–167.